Construction and Building Materials 409 (2023) 134074

Contents lists available at ScienceDirect

Construction and Building Materials

journal homepage: www.elsevier.com/locate/conbuildmat

Reaction kinetics and properties of pumice-based geopolymer systems cured at room temperature

Enver Küçükyıldırım [a], Hediye Yorulmaz [b], Ugur Durak [c], Serhan Ilkentapar [c], Burak Uzal [b], Okan Karahan [c,*], Cengiz Duran Atis [c]

[a] Graduate School of Natural and Applied Science, Erciyes University, 38280 Kayseri, Türkiye
[b] Civil Engineering Department, Abdullah Gül University, 38080 Kayseri, Türkiye
[c] Civil Engineering Department, Erciyes University, 38280 Kayseri, Türkiye

ARTICLE INFO

Keywords:
Pumice
Reaction kinetics
Room temperature
Geopolymer paste

ABSTRACT

This research investigated the kinetics of pumice-based geopolymer systems and their physical and mechanical properties. The effect of the Na_2SiO_3/NaOH ratio of geopolymer systems on the rate of heat evolution and total heat of reaction were examined via isothermal calorimetry of geopolymer pastes prepared with Na_2SiO_3/NaOH ratios of 2.5, 3, and 3.5. Hardened pastes were also studied with thermo-gravimetric analysis to determine weight loss. In addition, the unit weights and compressive strengths of the pastes prepared using pumice were measured. Although the hydration process starts the earliest in pumice-based geopolymer pastes with a Na_2SiO_3/NaOH ratio of 2, they have the lowest total hydration temperature. Na_2SiO_3/NaOH ratio of 2.5 by mass, shows higher weight loss obtained from TGA results. The compressive strength of the paste sample, prepared with a Na_2SiO_3/NaOH ratio of 3.5 by mass, was the highest, with 36.30 MPa at 28d. Depending on the Na2SiO3/NaOH ratio, it is thought that as the amount of Na2SiO3 increases in the samples, silica gel formation increases in later ages.

1. Introduction

Due to the cement and concrete industry's adverse effects on nature, an alternative binding system to traditional cementitious systems has been investigated. As a result of the research, it has been observed that it is possible to obtain binder systems with inorganic polymeric structures due to the reaction of reactive Al_2O_3, SiO_2, and CaO amorphous materials in the material's structure with alkaline solutions. As a result of the reaction of aluminosilicate fly ash with activators, an amorphous inorganic polymer called "Geopolymer" is formed [1]. As the aluminosilicate network is formed, the oxygen atom of the SiO_4 and AlO_4 tetrahedral structural unit is shared. In order to keep the negative ion charge of the aluminum in balance, positive ion structures such as Ca^{2+}, K^+, and Na^+ must exist [2]. It has been stated that it is possible to examine the geopolymerization mechanism in three stages. In the first stage, dissolving the binding material of the alkaline solution takes place. In the second stage, the compatibility of dissolved species with each other occurs. In the third stage, polycondensation occurs to form polymeric network structures [3]. While using geopolymer binders in concrete production offers an alternative nature-friendly material, it plays a vital role in reducing the carbon emissions released into the environment due to not using cement [4]. Sustainability, which is gaining increasing importance due to the widespread usage of geopolymer binders, is also ensured. Compared to traditional concrete, geopolymer concrete is essential sustainability in the construction sector by reducing the energy cost and carbon emissions stemming from cement usage in the concrete and ensuring waste disposal arising from by-products usage. The cement industry is responsible for about 7 % of the world's global CO_2 emissions [5,6,7]. The range of CO_2 values reported for geopolymer systems is estimated to be up to 80 % lower than Portland cement [8]. The difference is striking; geopolymers can be called environmentally friendly systems. When the properties of Portland cement and geopolymers are compared, geopolymer systems can gain compressive strength faster and provide better resistance to acid attacks [9,10]. Geopolymer systems provide strength and durability as well as sustainability [11]. In addition, the advantages of geopolymer systems include fire resistance [12,13,14] and resistance to chemical attacks [15,16,17,18].

* Corresponding author.
E-mail address: okarahan@erciyes.edu.tr (O. Karahan).

https://doi.org/10.1016/j.conbuildmat.2023.134074
Received 24 August 2023; Received in revised form 30 October 2023; Accepted 2 November 2023
Available online 20 November 2023

The two significant needs for geopolymers are source materials and an alkali-activating solution. The resource materials should include aluminosilicate [19]. Therefore, resource materials can be blast furnace slag [20,21,22,23,24], fly ash [11,25,26,27], metakaolin [28,29,30,31], volcanic ash [18,32,33], and silica fume [17,34]. In addition to these precursors, the research for new precursors as raw materials in geopolymer production has started. Pumice is also a raw material that has recently attracted the attention of researchers [35,36,37,38].

Volcanic pumice is a natural building material formed due to rapid cooling of molten lava [39]. Gas-filled foamy magma rapidly cools and solidifies as an amorphous porous rock [40]. Due to the vesicular structure of volcanic pumice, it is easier to process [41]. The structure of pumice is amorphous and contains a high amount of silica. When finely ground, it shows excellent pozzolanic properties [36]. Szabó et al. noted encouraging results when using pumice in geopolymer systems, indicating the potential of using pumice as alternative geopolymer precursor [40].

The Paris Climate Agreement (March 2021) aimed to reduce the long-term temperature target of a global average temperature increase from pre-industrial levels. It aimed to reduce the increment level from around 2℃ to around 1.5 ℃. If this target is met, it is estimated that the risks of climate change will decrease. Within the scope of this agreement, each country should determine a target for CO_2 emissions and be in a better condition than these determined goals every year. Contrary to the Kyoto Protocol published in 1997, this agreement obliges developed and developing countries to reduce CO_2 emissions [42]. It is obvious that pumice-based geopolymers, which minimize the adverse environmental effects and are intended to be used as eco-friendly building materials, will benefit economically, considering the rich reserve resources of Türkiye [43].

Silva et al. [44] investigated the reaction kinetics at early ages in geopolymer systems using metakaolin. Since the rate of condensation between silicate types is slower than between aluminate and silicate types, they found that setting occurs later with increasing silicate content. Although the formation of aluminate geopolymer plays a vital role in regulating the setting time, the amount of silicate present is responsible for these systems developing higher strength later on.

Liang et al. [45] investigated the early reaction of metakaolin geopolymer prepared with activators with different silicate modules using NMR and isothermal calorimetry. As a result, they determined that the heat flow and the total heat released are high in geopolymers with low silicate modulus.

Provis and Rees [46] stated that in keeping with geopolymerization kinetics, existing techniques could not explain the reaction process; therefore, new techniques should be developed.

Hattaf et al. [47] investigated the reaction kinetics of metakaolin and fly ash-based geopolymers.

When the publications in the literature are examined, it has been determined that there are deficiencies in examining the reaction kinetics of pumice-based geopolymers. The present study aims to contribute to the literature. The mechanical properties of pumice-based geopolymer pastes were investigated. Na_2SiO_3 and NaOH were used together as an alkali activator. Pumice-based geopolymer paste systems with Na_2SiO_3/NaOH (by mass) 2.5, 3, and 3.5 ratios were prepared and cured in the air until the day of the experiment. Isothermal calorimetry test, Thermogravimetric analysis (TGA), unit weight test, compressive strength test, SEM, and EDX analysis were performed on the prepared specimens, and the properties of the systems were determined and evaluated following the results of these tests.

2. Materials and methods

2.1. Materials

The pumice used in this study was obtained from Nevşehir, Türkiye. The pumice's chemical composition and XRD pattern are given in Table 1 and Fig. 1, respectively. As seen in Fig. 1, pumice has an amorphous structure, indicated by the raised background. The sodium hydroxide flakes and sodium metasilicate, having 98.4 % and 95 % purity, respectively, were used as alkali activators.

2.2. Methods

In the mixture design, water/pumice ratios in the samples were determined by providing appropriate flow values. The w/b ratio was kept constant at 0.8 in the paste samples (except for the isothermal calorimeter test) prepared from pumice (P). Drinkable tap water was used in this study. Also, some trial mixtures were made, within the scope of the trial studies, no strength could be obtained in the specimens produced with a Na/Al ratio of 1 (50 g Na2SiO3 and 20 g NaOH activator and 450 g pumice). In addition, no significant strength could be measured in specimens produced with a Na/Al ratio of 2 (100 g Na2SiO3 and 40 g NaOH and 450 g pumice). For this reason, the Na/Al ratio was taken as 4 and the study was carried out using the mixture ratios given in Table 2. Detailed information about the mixture proportion is given in Table 2. Paste samples were prepared using a laboratory mixer. The NaOH solution diluted with water for the mixtures was prepared in glass jars and kept at room temperature for one day. The prepared NaOH solution was added to the dry mixture and put into the mixer. While preparing the paste, the mixtures to which the solution was added were mixed for 60 s at low speed. Then, the mixer was run at high speed and mixing was done for another 60 s. When 120 s were completed, the mixer was stopped. The produced geopolymer pastes were poured into prismatic molds of 40 mm x 40 mm x 160 mm in two layers and placed on the vibration table after each layer to ensure the samples were well compacted. Trial studies were carried out for curing conditions (wet or dry). Strength was not obtained when the specimens were cured by placing them in water immediately after being removed from the mold. Therefore, air curing method was preferred in the study. However, no significant strength loss was observed when the 28-day air-cured specimens were placed in water.

The samples in the molds were kept in air for 1, 2, 3, 7 and 28 days under ambient conditions. Unit weight and compressive strength were measured at each curing time according to ASTM C642 [48] and TS EN 1015–11 [49], on six samples, respectively. The water/pumice ratio was selected for the isothermal calorimetry tests as 0.7, and geopolymer pastes were prepared at the same and constant w/b. Pumice-based geopolymer pastes were assessed for 72 h at 25 °C. Before the compressive strength test, the weights of air-cured specimens were measured, in this way unit weight was determined. Thermal analysis of pumice-based geopolymer samples was performed with DT-TGA device (DTG-60H TGA, Shimadzu). The experiment was conducted with a heating rate of 15 °C/min for the temperature range from ambient temperature to 1000 °C.

3. Results and discussion

3.1. Isothermal calorimetry test

Isothermal calorimetry tests were performed on the pumice-based

Table 1
Chemical composition of Pumice Powder (%).

	SiO_2	Al_2O_3	Fe_2O_3	Na_2O	K_2O	MgO	TiO_2	SO_3	$CaCO_3$	BaO
Pumice	76.08	12.46	1.327	1.181	4.741	<0.051	0.1718	<0.048	1.371	0.02756

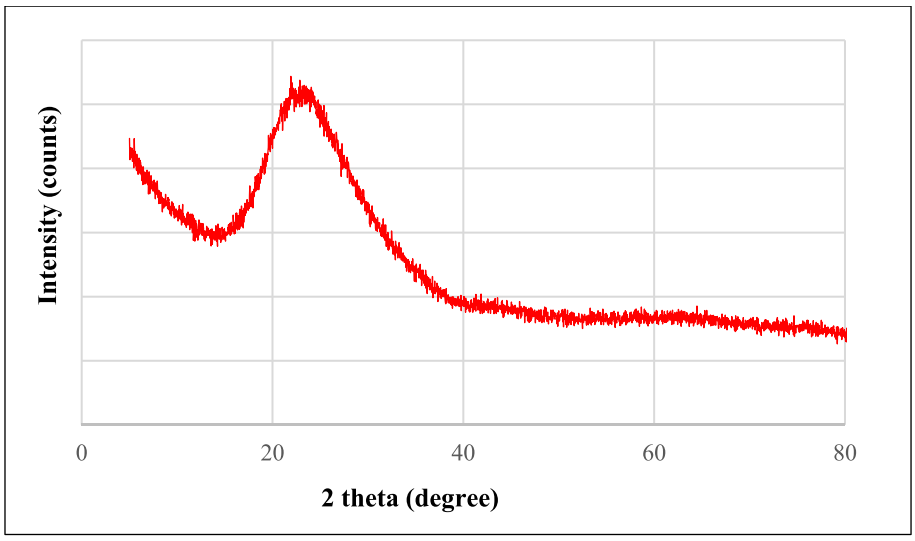

Fig. 1. XRD pattern of pumice.

Table 2
Mix design of geopolymer pastes.

Specimen code	Na_2SiO_3/NaOH (By mass)	Pumice (g)	Na_2SiO_3 (g)	NaOH Solution	
				Water (g)	NaOH (g)
2.5PM	2.5	450	200	365	80
3PM	3	450	240	365	80
3.5PM	3.5	450	280	365	80

geopolymer pastes for 24 h at 25 °C, and test results are presented in Figs. 2 and 3. According to Fig. 2, paste coded 3PM has a higher rate of hydration than the others. On the other hand, the hydration rate of 3.5PM is remarkably close to 3PM. Maximum hydration rates of 2.5 PM, 3 PM, and 3.5 PM are 64 mW/g, 78 mW/g, and 91 mW/g, respectively. Besides, it was observed that hydration started later as the Na_2SiO_3/NaOH ratio increased. When the experimental results are analyzed according to Fig. 2, it is clear that the hydration heat values range between 144 J/g to 155 J/g. As can be seen, the 3 PM has the highest heat of hydration. Although 2.5 PM is the sample whose hydration starts first, the total heat of hydration value is lower than the other two samples. According to these results, it can be said that the hydration process is slower in samples with a Na_2SiO_3/NaOH ratio of 2.5 compared to a higher Na_2SiO_3/NaOH ratio.

3.2. TGA/DTA

TGA/DTA was performed on pumice-based geopolymer samples on the 1st day and 3rd day. The results of TGA are presented in Figs. 4 and 5. A rapid decrease in weight up to 120 °C occurred, associated with the evaporation of free water with increasing temperature. Although there was a weight reduction at 100–500 °C in all samples, it was slower compared to the first stage. After 500 °C, the weight reduction became much smaller, and the curve became almost horizontal. A decrease between 138 °C and 500 °C is thought to be a result of the evaporation of the water trapped in the N-A-S-H and gel pores up to approximately 138 °C-300 °C.

It can also be expressed as the dehydroxylation of the hydrated gel [50–52]. According to the literature, the weight loss above 300 °C in the TGA data is attributed to the dehydration of the chemically bound water [53]. Ranjbar stated in his study that TGA on FA/Palm oil fuel ash-based geopolymers was conducted in four stages. These stages can be listed as follows; evaporation of water and OH groups; decomposition of geopolymer components such as $Ca(OH)_2$; transformation to the nepheline stage; and the last stage where the weight losses do not change [53]. In this study, the reduction at approximately 138 °C can be considered as the evaporation of water added to prepare the solution before the geopolymerization step. This situation can be considered as water evaporation in the pores above 5 nm, as Škvára et al. stated [54]. Weight losses between 300 °C and 400 °C show similar behavior to chemically bound water dehydration. The crystallization of iron oxide can explain the weight loss between 400 °C and 500 °C. Weight losses between 138 °C

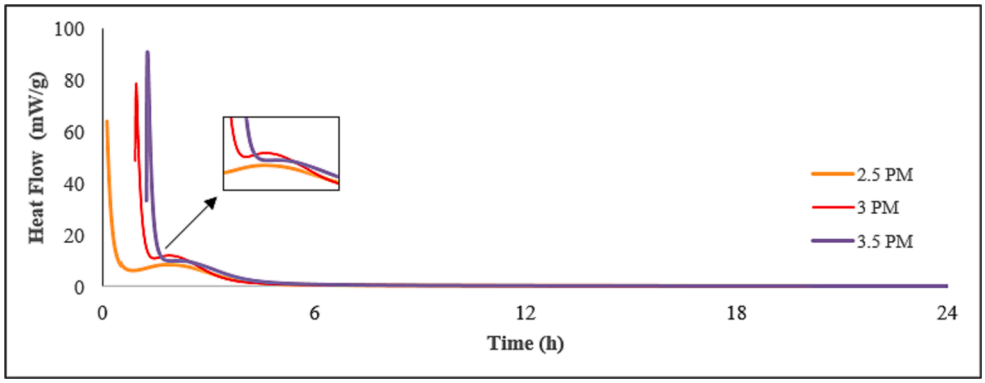

Fig. 2. The rate of the hydration of pumice-based geopolymer pastes.

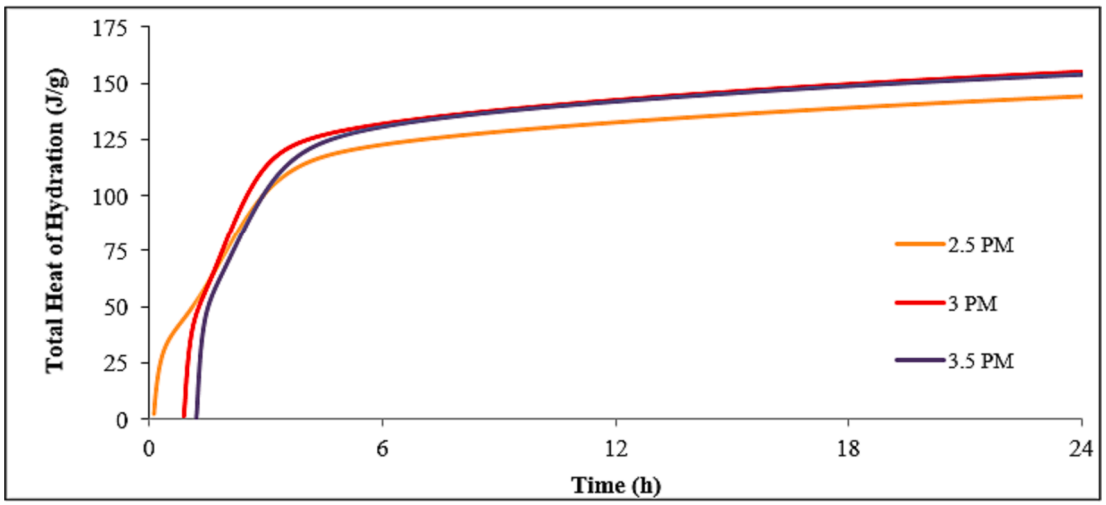

Fig. 3. The total heat of the reaction of pumice-based geopolymer pastes.

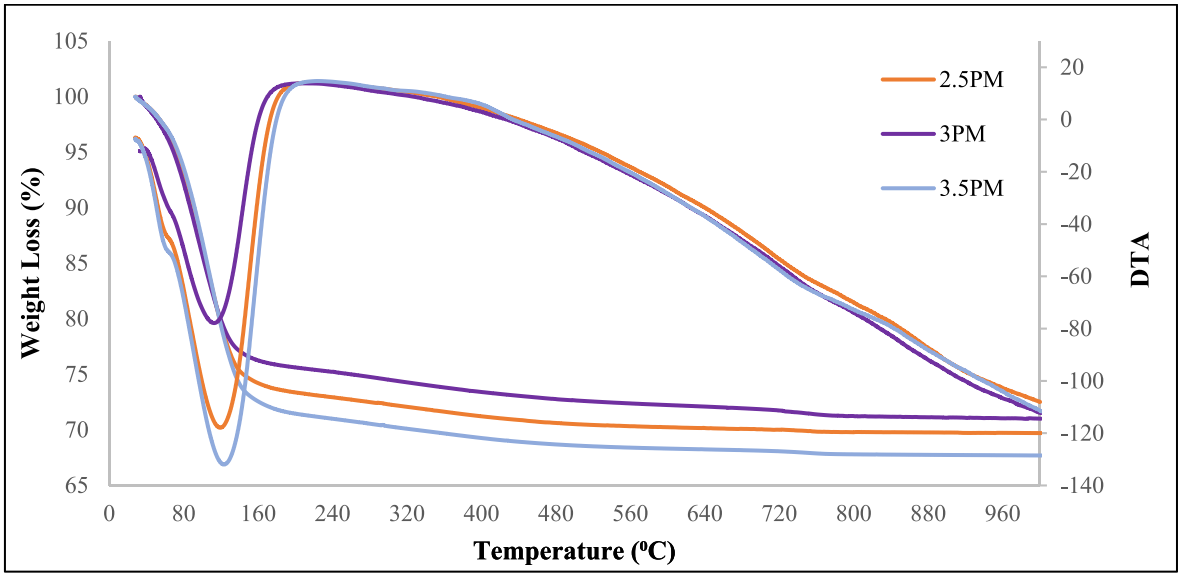

Fig. 4. Weight (%) and DTA of pumice-based geopolymer paste samples on day 1-day.

and 500 °C are considered as the evaporation of the bound waters in the hydroxyl groups during phase changes [53]. This aligns with our TGA analysis's behavior between 138 °C and 500 °C. The decrease between 500 °C and 800 °C is caused by the losses in the conversion stage to the nepheline stage. It consists of the phases of being constant between 800 °C and 1000 °C. Nath et al. stated that in the TGA analysis of FA used in three different sizes, fine materials are more reactive, and therefore, the added alkali solution is primarily consumed in the forming of N-A-S-H gel. They reported that this situation reduces the amount of CO_2 penetrating the geopolymer matrix [50]. Based on Figs. 4 and 5, while the temperature was between 120ºC-1000ºC, weight loss in 1-day 2.5PM, 3PM and 3.5PM, samples were observed as 8.02 %, 6.35 %, and 7.95 % respectively. In the 3-day 2.5PM, 3PM and 3.5PM, samples, weight loss was observed as 8 %, 6.95 % and 6.81 %, respectively. Weight loss in the 2.5 PM sample remained almost the same on the 3rd day compared to the 1st day.. While the weight loss increased in 3PM, it decreased in 3.5 PM sample.

3.3. Unit weight test

The unit weights of hardened geopolymer samples are presented in Fig. 6. Per Fig. 6, the mixture coded 2.5PM specimens have the lowest value in unit weight for all ages. For instance, the unit weight test on the 1st day, it was found to be 1.63 t/m^3, 1.66 t/m^3, and 1.67 t/m^3 for 2.5 PM, 3PM, and 3.5 PM, respectively. Unit weight values on day 7 were 1.68 t/m^3, 1.70 t/m^3, and 1.73 t/m^3 for 2.5 PM, 3PM, and 3.5 PM, respectively. It was detected that the unit weight increased slightly in the samples prepared by increasing the amount of Na_2SiO_3/NaOH by mass. This increment is believed to result from the fact that the unit weight of the solution increases while the Na_2SiO_3/NaOH rate increases. Therefore, the unit weight of geopolymer samples increases with the Na_2SiO_3/NaOH rate increase. Moreover, it can be seen from Fig. 6 that the unit weight of geopolymer samples increases with the increase of air curing time. This increment in curing time is thought to be due to the fact that the reaction with the geopolymer pastes by taking CO_2 from the air and forming a Na_2CO_3 structure; the longer the curing time is, the more carbonation reaction occurs.

3.4. Compressive strength test

The compressive strengths of the samples are shown in Fig. 7. Based on Fig. 7, the compressive strength on the 1st day was 1.0, 1.2 and 2.3

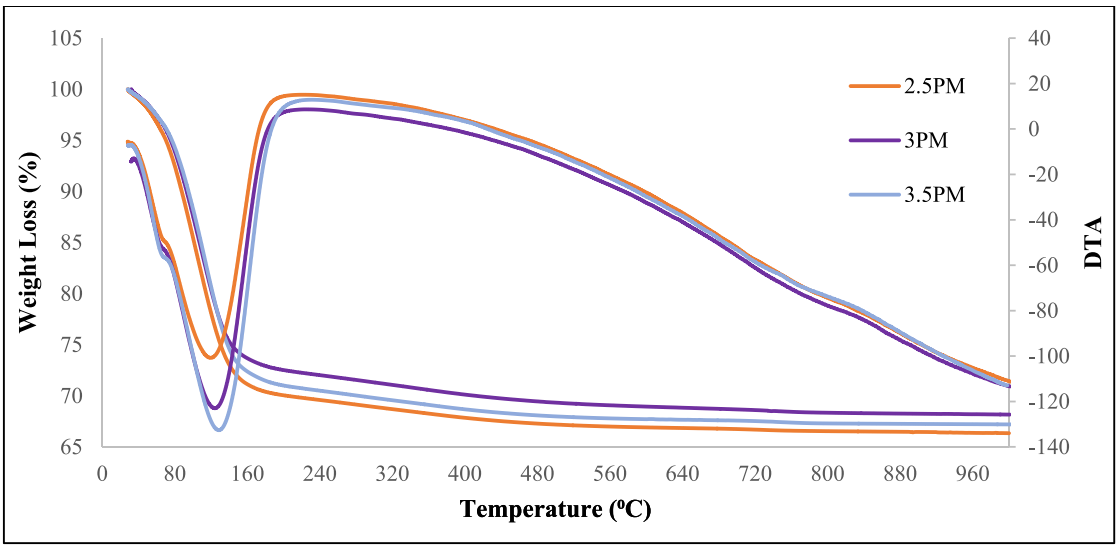

Fig. 5. Weight (%) and DTA of pumice-based geopolymer paste samples at 3-day.

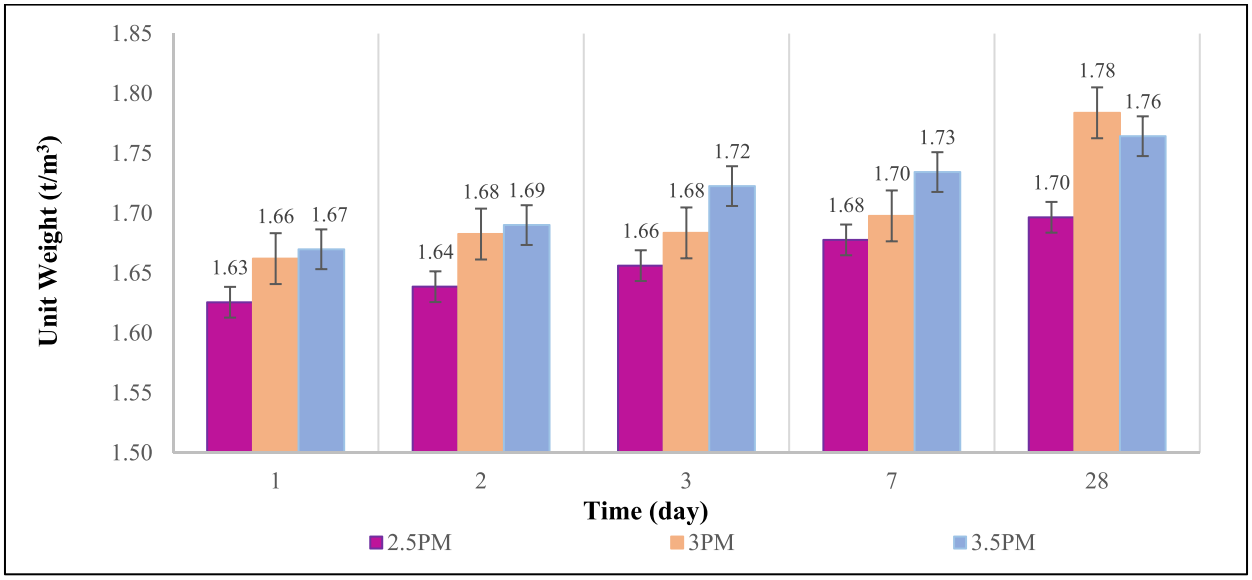

Fig. 6. Unit weight of geopolymer paste samples at different ages.

MPa for 2.5PM, 3 PM and 3.5 samples. The compressive strength on the 2nd day was determined as 1.4, 1.7, and 2.6 MPa for the 2.5PM, 3 PM and 3.5 PM sample. The compressive strength on the 3rd day was determined as 1.9, 2.6, and 2.9 MPa for the 2.5PM, 3 PM, and 3.5 PM samples. The compressive strength on the 7th day was determined as 3.8, 4.0, and 5.8 MPa for the 2.5PM, 3 PM, and 3.5 PM samples. The compressive strength at 28 days was noted as 11.0 MPa, 17.4 MPa, and 36.3 MPa for 2.5PM, 3PM, and 3.5PM, respectively. It has been observed that the increase in the Na_2SiO_3/NaOH ratio has a positive effect on the compressive strength of the system at all ages.

3.5. SEM and EDX analysis

SEM images of geopolymers at on day 1, day 3, and day 28 for 2,5PM, 3PM, and 3,5PM samples are shown in Fig. 8 and EDX analysis of geopolymer samples at 28 days is given in Fig. 9. SEM images show pores, geopolymer gel, and non-reacted powder particles of geopolymer samples. The SEM images of the mixtures show clear differences between curing time and mixtures. In the 1-day and 3-day SEM images of the prepared paste samples, a large number of partially reacted and unreacted pumice particles, stated a low dissolution with the geopolymer gel, which is non-compact, porous, and has a brittle surface, are seen. Similar observation has also been made by other researchers [35]. On the other hand, a denser and more uniform microstructure with a few unreacted precursor particles is shown in 28-day SEM images. According to 28-day SEM images, it also coincides with the EDX analysis results in Fig. 9, where the geopolymerization is more in the 3.5PM sample and has a denser structure. Elemental component amounts of geopolymer pastes are determined using SEM-EDX by performing mapping analysis on their surfaces. Pumice powder's primary elemental components are Si, Na, and Al. These elements show that an amorphous alkali aluminosilicate gel is the product of geopolymerization [35,55,56]. Thus, the increase in compressive strength of the 3.5PM paste sample was supported by SEM pictures and the EDX analysis results.

The Si/Na or Si/K atomic ratios of the alkaline solution significantly affect the degree of polymerization of the dissolved material [57,58]. It has been reported in previous studies that the compressive strength increases with the rise of Si/Na ratios up to a specific ratio. Comparable

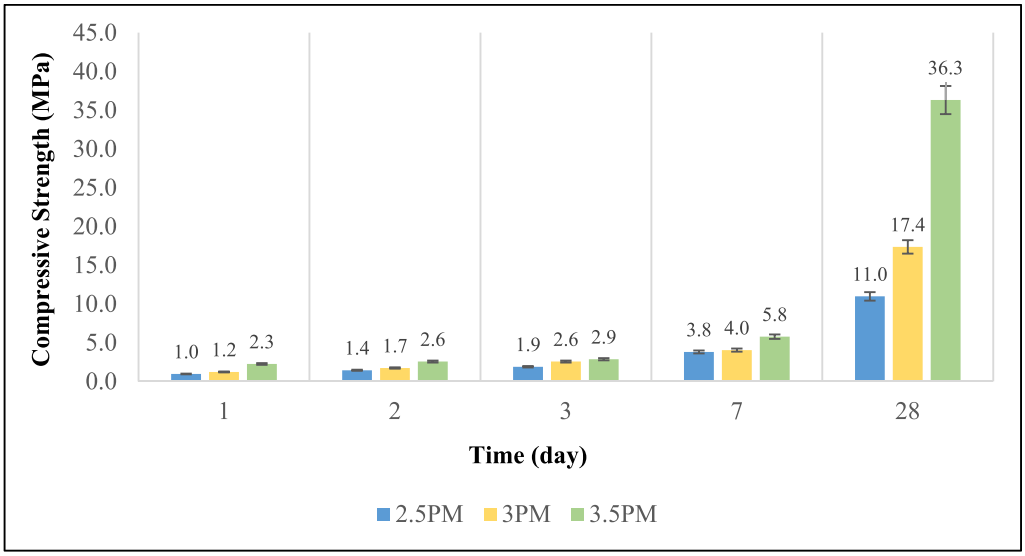

Fig. 7. Compressive strength of geopolymer paste samples.

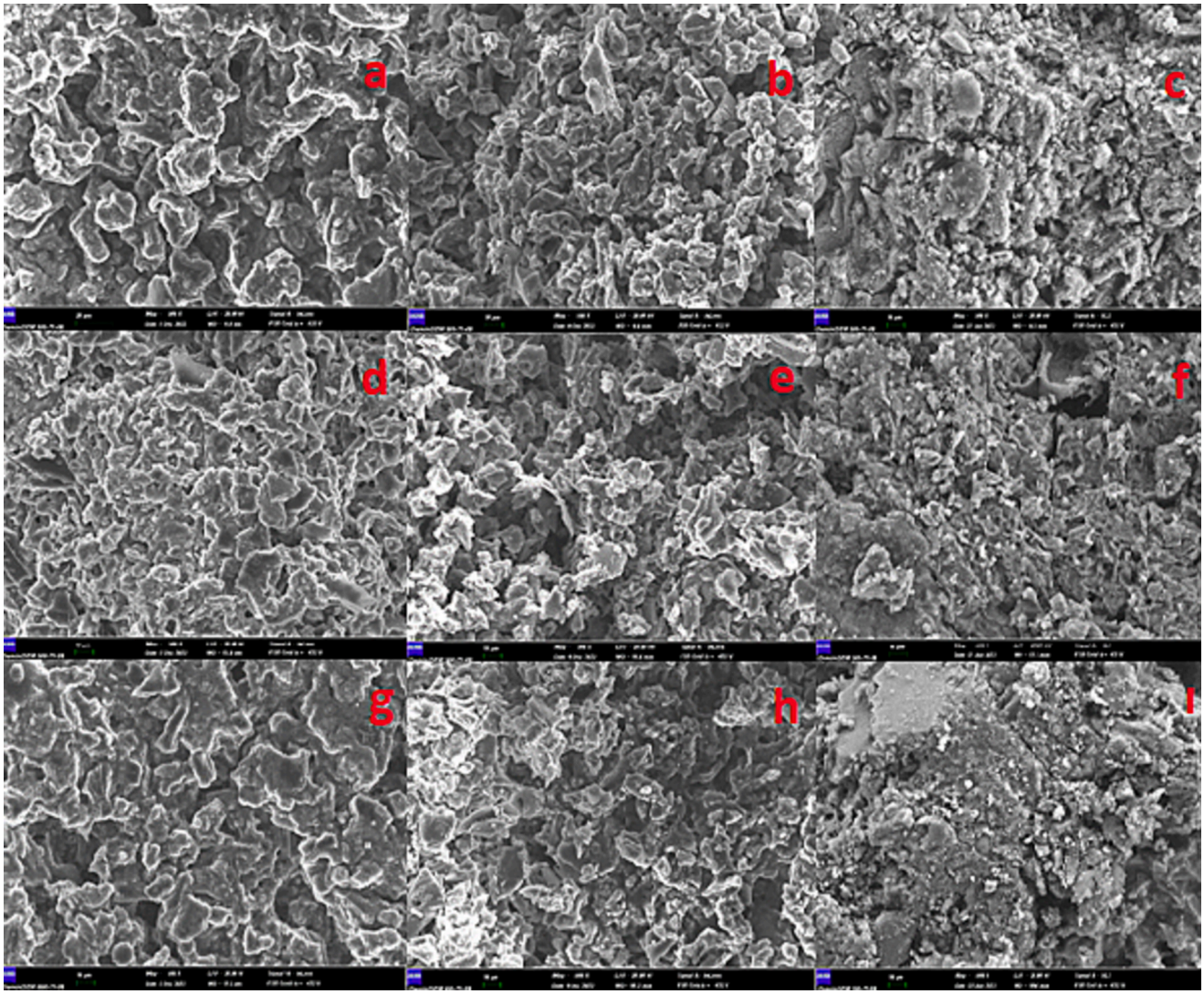

Fig. 8. SEM images (500x). 2.5PM 1-day (a), 3-day (b), 28-day (c); 3PM 1-day (d), 3-day (e), 28-day (f); 3.5PM 1-day (g), 3-day (h), 28-day (i).

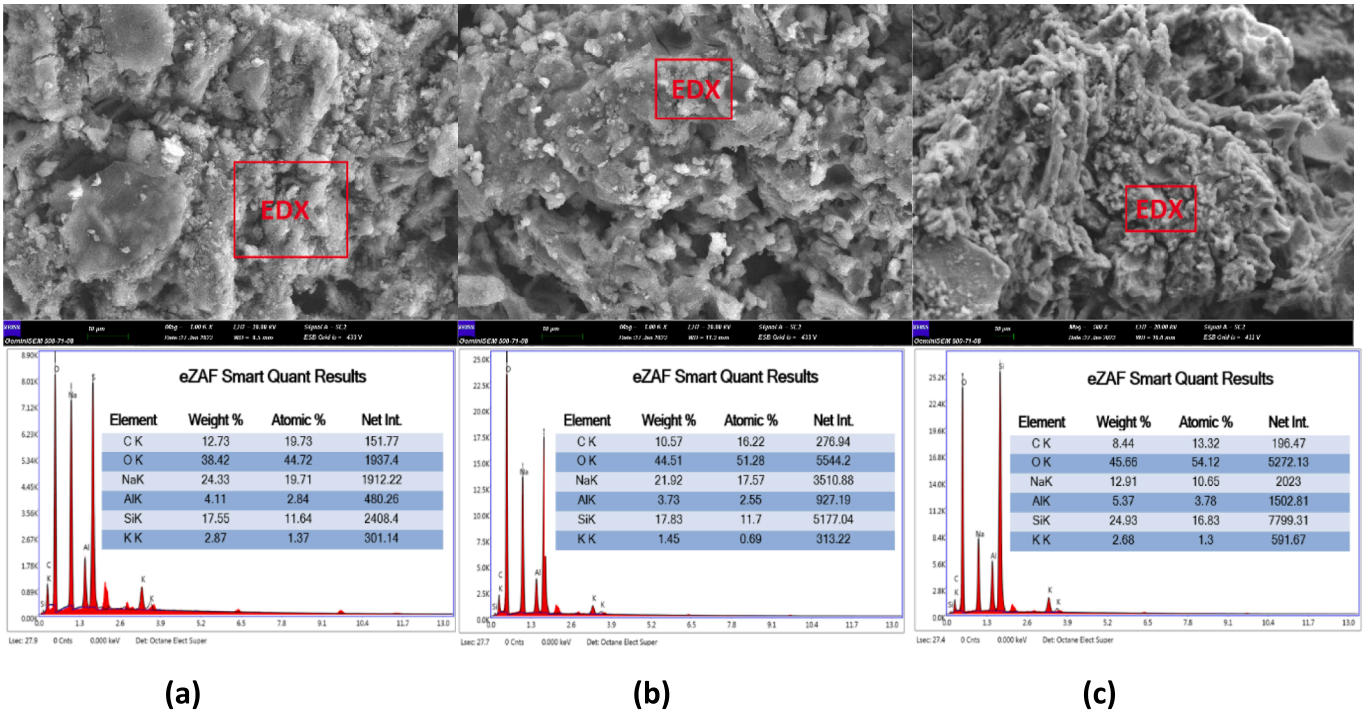

Fig. 9. EDX results at 28-day 2.5PM (a)-3PM (b)-3.5PM (c).

results are seen in this study as well. Accordingly, the compressive strengths of the 3.5PM, 3PM, and 2.5PM samples were obtained as 36.3, 17.4, and 11.0 MPa, respectively, while the Si/Na ratios were obtained as 1.59, 0.67, and 0.59, respectively.

The geopolymer gel structure formed in Fig. 8 (i) and the geopolymerized pumice grains bonded to each other show a quite different microstructure from Fig. 8 (c) and (f), and nearly all of the sodium crystals were consumed in the geopolymerization reactions. This situation also explains the Si/Na ratio (1.59) and 28-day compressive strength results according to the EDX results.

5. Conclusion

This study investigated the geopolymerization of pumice using Na_2SiO_3/NaOH at different mass ratios. As a result of the study, the following results were obtained;

1) According to the isothermal calorimetry test, although the pumice-based geopolymer pastes with a Na2SiO3/NaOH ratio of 2.5 began the hydration process earlier, its total heat of hydration is the lowest. Paste samples with a Na_2SiO_3/NaOH ratio of 3 and 3.5 showed remarkably similar values. As a result of the increase in the Na_2SiO_3/NaOH ratio by mass, the Na_2O content increased. The increment in Na_2O content caused shifts in the peaks, indicating the dissolution-gelling state.
2) Based on the TGA test, weight loss up to 120 °C is thought to be due to free water. At higher temperatures, on the 1-day results, the highest weight loss was observed at 3.5PM, 2.5PM, and 3PM, respectively. However, the 3-day results showed that the highest weight loss was at 3.5PM, 3PM, and 2.5PM, respectively. The decrement in weight loss is thought to be due to the deterioration of the geopolymer gels.
3) The unit weight of geopolymer samples increases not only the rise of Na_2SiO_3/NaOH rate but also curing time.
4) The highest 28-day compressive strength was obtained in the paste sample prepared with a Na_2SiO_3/NaOH ratio of 3.5 by mass. Since more sodium silicate is used, more silica gel is formed, thus providing the highest strength.
5) A non-compact, porous structure of many unreacted and partially reacted pumice particles was observed in the SEM images at early ages. However, a denser and more homogeneous structure was observed in the following days. According to the EDX results, it was observed that the 3.5PM sample had the densest microstructure and, thus, the highest strength.

CRediT authorship contribution statement

Enver Küçükyıldırım: Investigation. **Hediye Yorulmaz:** Visualization. **Ugur Durak:** Writing – original draft. **Serhan Ilkentapar:** Investigation. **Burak Uzal:** Resources, Supervision. **Okan Karahan:** Resources, Project administration. **Cengiz Duran Atiş:** Writing – review & editing.

Declaration of Competing Interest

The authors declare the following financial interests/personal relationships which may be considered as potential competing interests: Okan KARAHAN reports financial support was provided by Erciyes University. Okan KARAHAN reports a relationship with Erciyes University that includes: funding grants.

Data availability

Data will be made available on request.

Acknowledgement

Erciyes University, Scientific Research Project Coordination Unit, supported this work with project code FDK-2022-11921.

References

[1] S. Aydın, "Alkalilerle Aktive Edilmiş Yüksek Fırın Cürufu Bağlayıcılı Lifli Kompozit Geliştirilmesi," *Dokuz Eylül üniversitesi Fen Bilim. Enstitüsü Doktora Tezi*, p. 330 sf, 2010.

[2] A. Allahverdi, K. Mehrpour, E. Najafikani, Investigating the possibility of utilizing pumice-type natural pozzonal in production of geopolymer cement, Ceram. - Silikaty 52 (1) (2008) 16–23.

[3] N. Davidovits, J., Davidovics, M., Davidovits, "Process for Obtaining a Geopolymeric Alumino-Silicate And Products Thus Obtained," . *U.S. Pat. no. 5,342,595*, 1994.

[4] A. Wongsa, V. Sata, P. Nuaklong, P. Chindaprasirt, Use of crushed clay brick and pumice aggregates in lightweight geopolymer concrete, Constr. Build. Mater. 188 (2018) 1025–1034, https://doi.org/10.1016/j.conbuildmat.2018.08.176.

[5] H. Hakkomaz, H. Yorulmaz, U. Durak, S. İlkentapar, O. Karahan, C.D. Atiş, The influence of cement kiln dust on strength and durability properties of cement-based systems, Environ. Sci. Pollut. Res. (2022), https://doi.org/10.1007/s11356-022-21281-z.

[6] C.D. Atiş, E.B. Görür, O. Karahan, C. Bilim, S. Ilkentapar, E. Luga, Very high strength (120 MPa) class F fly ash geopolymer mortar activated at different NaOH amount, heat curing temperature and heat curing duration, Constr. Build. Mater. 96 (2015) 673–678, https://doi.org/10.1016/j.conbuildmat.2015.08.089.

[7] H. Yorulmaz, B. Uzal, O. Karahan, U. Durak, S. İlkentapar, C.D. Atiş, Effect of Nano-SiO2 on Strength and Hydration Characteristics of Ternary Cementitious Systems, Arab. J. Sci. Eng. (2023), https://doi.org/10.1007/s13369-023-07949-9.

[8] N. Kabay, M. Mert, N. Miyan, and T. Omur, "Pumice as Precursor in Geopolymer Paste and Mortar," *J. Civ. Eng. Constr.*, vol. 10, no. 4, pp. 225–236, 2021, 10.32732/jcec.2021.10.4.225.

[9] J. Davidovits, Geopolymers and geopolymeric materials, J. Therm. Anal. 35 (1989) 429–441.

[10] Z. Yunsheng, S. Wei, L. Zongjin, Composition design and microstructural characterization of calcined kaolin-based geopolymer cement, Appl. Clay Sci. 47 (3–4) (2010) 271–275, https://doi.org/10.1016/j.clay.2009.11.002.

[11] U. Durak, O. Karahan, B. Uzal, S. İlkentapar, C.D. Atiş, Influence of nano SiO2 and nano CaCO3 particles on strength, workability, and microstructural properties of fly ash-based geopolymer, Struct. Concr. 22 (S1) (2021) E352–E367, https://doi.org/10.1002/suco.201900479.

[12] O.A. Abdulkareem, A.M. Mustafa Al Bakri, H. Kamarudin, I. Khairul Nizar, A. A. Saif, Effects of elevated temperatures on the thermal behavior and mechanical performance of fly ash geopolymer paste, mortar and lightweight concrete, Constr. Build. Mater. 50 (2014) Jan, https://doi.org/10.1016/j.conbuildmat.2013.09.047.

[13] M. Lahoti, K.H. Tan, E.-H. Yang, A critical review of geopolymer properties for structural fire-resistance applications, Constr. Build. Mater. 221 (Oct. 2019), https://doi.org/10.1016/j.conbuildmat.2019.06.076.

[14] M. Amran, S. S. Huang, S. Debbarma, and R. S. M. Rashid, "Fire resistance of geopolymer concrete: A critical review," *Constr. Build. Mater.*, vol. 324, no. October 2021, p. 126722, 2022, 10.1016/j.conbuildmat.2022.126722.

[15] O.F. Nnaemeka, N.B. Singh, Durability properties of geopolymer concrete made from fly ash in presence of Kaolin, Mater. Today Proc. 29 (2019) 781–784, https://doi.org/10.1016/j.matpr.2020.04.696.

[16] A. Siddika, A. Hajimohammadi, M.A. Al Mamun, R. Alyousef, W. Ferdous, Waste glass in cement and geopolymer concretes: A review on durability and challenges, Polymers (basel) 13 (13) (2021) 1–26, https://doi.org/10.3390/polym13132071.

[17] S. Jena, R. Panigrahi, P. Sahu, Mechanical and Durability Properties of Fly Ash Geopolymer Concrete with Silica Fume, J. Inst. Eng. Ser. A 100 (4) (2019) 697–705, https://doi.org/10.1007/s40030-019-00400-z.

[18] P. N. Lemougna, U. F. Chinje Melo, M.-P. Delplancke, and H. Rahier, "Influence of the activating solution composition on the stability and thermo-mechanical properties of inorganic polymers (geopolymers) from volcanic ash," *Constr. Build. Mater.*, vol. 48, pp. 278–286, Nov. 2013, 10.1016/j.conbuildmat.2013.06.089.

[19] M. A. Hamid, N. Yaltay, and M. Türkmenoğlu, "Properties of pumice-fly ash based geopolymer paste," *Constr. Build. Mater.*, vol. 316, no. August 2021, pp. 1–10, 2022, 10.1016/j.conbuildmat.2021.125665.

[20] D. Bondar, S. Nanukuttan, J.L. Provis, M. Soutsos, Efficient mix design of alkali activated slag concretes based on packing fraction of ingredients and paste thickness, J. Clean. Prod. 218 (2019) 438–449, https://doi.org/10.1016/j.jclepro.2019.01.332.

[21] I. Amer, M. Kohail, M.S. El-Feky, A. Rashad, M.A. Khalaf, A review on alkali-activated slag concrete, Ain Shams Eng. J. 12 (2) (2021) 1475–1499, https://doi.org/10.1016/j.asej.2020.12.003.

[22] S. Aydın, B. Baradan, Effect of activator type and content on properties of alkali-activated slag mortars, Compos. Part B 57 (2014) 166–172, https://doi.org/10.1016/j.compositesb.2013.10.001.

[23] M.M. Alonso, F. Puertas, B. Gonz, "alkali-Activated Slag Concrete : Fresh and Hardened Behaviour" 85 (2018) 22–31, https://doi.org/10.1016/j.cemconcomp.2017.10.003.

[24] C.S. Thunuguntla, T.D. Gunneswara Rao, Effect of mix design parameters on mechanical and durability properties of alkali activated slag concrete, Constr. Build. Mater. 193 (2018) 173–188, https://doi.org/10.1016/j.conbuildmat.2018.10.189.

[25] M. Amran, S. Debbarma, T. Ozbakkaloglu, Fly ash-based eco-friendly geopolymer concrete: A critical review of the long-term durability properties, Constr. Build. Mater. 270 (2021), 121857, https://doi.org/10.1016/j.conbuildmat.2020.121857.

[26] L.N. Assi, E. Eddie, M.K. Elbatanouny, P. Ziehl, Investigation of early compressive strength of fly ash-based geopolymer concrete, Constr. Build. Mater. 112 (2016) 807–815, https://doi.org/10.1016/j.conbuildmat.2016.03.008.

[27] C.D. Atiş, High-volume fly ash concrete with high strength and low drying shrinkage, J. Mater. Civ. Eng. 15 (2) (2003) 153–156, https://doi.org/10.1061/(ASCE)0899-1561(2003)15:2(153).

[28] M.L. Kumar, V. Revathi, Microstructural Properties of Alkali-Activated Metakaolin and Bottom Ash Geopolymer, Arab. J. Sci. Eng. 45 (5) (2020) 4235–4246, https://doi.org/10.1007/s13369-020-04417-6.

[29] H. Lahalle, V. Benavent, V. Trincal, T. Wattez, R. Bucher, M. Cyr, Robustness to water and temperature, and activation energies of metakaolin-based geopolymer and alkali-activated slag binders, Constr. Build. Mater. 300 (2021), 124066, https://doi.org/10.1016/j.conbuildmat.2021.124066.

[30] K. M. L. Alventosa and C. E. White, "The effects of calcium hydroxide and activator chemistry on alkali-activated metakaolin pastes," *Cem. Concr. Res.*, vol. 145, no. March, p. 106453, 2021, 10.1016/j.cemconres.2021.106453.

[31] A. Hasnaoui, E. Ghorbel, G. Wardeh, Effect of Curing Conditions on the Performance of Geopolymer Concrete Based on Granulated Blast Furnacefile:///C:/Users/Agu Asus Laptop/Downloads/1-s2.0-S0950061821036746-main.pdf file:///C:/Users/Agu Asus Laptop/Downloads/Final_Exam_Student_5.docx Slag a, J. Mater. Civ. Eng. 33 (3) (2021) 04020501, https://doi.org/10.1061/(asce)mt.1943-5533.0003606.

[32] P.N. Lemougna, U.F. Chinje Melo, M.-P. Delplancke, H. Rahier, Influence of the chemical and mineralogical composition on the reactivity of volcanic ashes during alkali activation, Ceram. Int. 40 (1) (Jan. 2014) 811–820, https://doi.org/10.1016/j.ceramint.2013.06.072.

[33] P.N. Lemougna, K.J.D. MacKenzie, U.F.C. Melo, Synthesis and thermal properties of inorganic polymers (geopolymers) for structural and refractory applications from volcanic ash, Ceram. Int. 37 (8) (Dec. 2011) 3011–3018, https://doi.org/10.1016/j.ceramint.2011.05.002.

[34] Y. C. Wang, X. Kou, J. Deng, J. P. Zhao, and H. Shi, "Ammonium polyphosphate/expandable graphite/TiO2 blended silica fume-based geopolymer coating for synergistically flame-retarding plywood," *Constr. Build. Mater.*, vol. 317, no. November 2021, p. 125941, 2022, 10.1016/j.conbuildmat.2021.125941.

[35] P. Nasaeng, A. Wongsa, R. Cheerarot, V. Sata, P. Chindaprasirt, "Strength enhancement of pumice-based geopolymer paste by incorporating recycled concrete and calcined oyster shell powders", Case Stud, Constr. Mater. vol. 17, no. March (2022) e01307.

[36] C. Karaaslan, E. Yener, T. Bağatur, R. Polat, R. Gül, M. Hakkı Alma, Synergic effect of fly ash and calcium aluminate cement on the properties of pumice-based geopolymer mortar, Constr. Build. Mater. 345 (June) (2022), https://doi.org/10.1016/j.conbuildmat.2022.128397.

[37] C. Karaaslan, E. Yener, T. Bağatur, R. Polat, Improving the durability of pumice-fly ash based geopolymer concrete with calcium aluminate cement, J. Build. Eng. 59 (April) (2022), https://doi.org/10.1016/j.jobe.2022.105110.

[38] B. Balun, M. Karataş, Influence of curing conditions on pumice-based alkali activated composites incorporating Portland cement, J. Build. Eng. 43 (January) (2021), https://doi.org/10.1016/j.jobe.2021.102605.

[39] D. Sari, A.G. Pasamehmetoglu, The effects of gradation and admixture on the pumice lightweight aggregate concrete, Cem. Concr. Res. 35 (5) (2005) 936–942, https://doi.org/10.1016/j.cemconres.2004.04.020.

[40] R. Szabó, F. Kristály, S. Nagy, R. Singla, G. Mucsi, S. Kumar, Reaction, structure and properties of eco-friendly geopolymer cement derived from mechanically activated pumice, Ceram. Int. 49 (4) (2023) 6756–6763, https://doi.org/10.1016/j.ceramint.2022.10.204.

[41] P.N. Lemougna, et al., Review on the use of volcanic ashes for engineering applications, Resour. Conserv. Recycl. 137 (June) (2018) 177–190, https://doi.org/10.1016/j.resconrec.2018.05.031.

[42] *United Nations Paris Climate Agreement.* .

[43] M.M. Yadollahi, A. Benli, R. Demirboła, The effects of silica modulus and aging on compressive strength of pumice-based geopolymer composites, Constr. Build. Mater. 94 (2015) 767–774, https://doi.org/10.1016/j.conbuildmat.2015.07.052.

[44] P. De Silva, K. Sagoe-Crenstil, V. Sirivivatnanon, Kinetics of geopolymerization: Role of Al2O3 and SiO2, Cem. Concr. Res. 37 (4) (2007) 512–518, https://doi.org/10.1016/j.cemconres.2007.01.003.

[45] G. Liang, W. Yao, and A. She, "New insights into the early-age reaction kinetics of metakaolin geopolymer by 1H low-field NMR and isothermal calorimetry," *Cem. Concr. Compos.*, vol. 137, no. July 2022, p. 104932, 2023, 10.1016/j.cemconcomp.2023.104932.

[46] J.L. Provis, C.A. Rees, Geopolymer synthesis kinetics, Geopolymers Struct. Process. Prop. Ind. Appl. (2009) 118–136, https://doi.org/10.1533/9781845696382.1.118.

[47] R. Hattaf, et al., Metakaolin and Fly Ash-based Matrices for Geopolymer Materials: Setting Kinetics and Compressive Strength, Silicon 14 (12) (2022) 6993–7004, https://doi.org/10.1007/s12633-021-01447-z.

[48] Astm c642–13,, Standard Test Method for Density, Absorption, and Voids in Hardened Concrete, ASTM, West Conshohocken, 2013.

[49] TS EN 1015-11, *Mortar Testing Method, Part 11. Measurement of Compressive and Flexural Tensile Strength of Mortar*. Ankara, Turkey: TSE, 2000.

[50] S.K. Nath, S. Kumar, Role of particle fineness on engineering properties and microstructure of fly ash derived geopolymer, Constr. Build. Mater. 233 (2020), 117294, https://doi.org/10.1016/j.conbuildmat.2019.117294.

[51] E.D. Rodríguez, S.A. Bernal, J.L. Provis, J. Paya, J.M. Monzo, M.V. Borrachero, Effect of nanosilica-based activators on the performance of an alkali-activated fly ash binder, Cem. Concr. Compos. 35 (1) (2013) 1–11, https://doi.org/10.1016/j.cemconcomp.2012.08.025.

[52] G. Görhan, G. Kürklü, The influence of the NaOH solution on the properties of the fly ash-based geopolymer mortar cured at different temperatures, Compos. Part B Eng. 58 (2014) 371–377, https://doi.org/10.1016/j.compositesb.2013.10.082.

[53] N. Ranjbar, M. Mehrali, U.J. Alengaram, H.S.C. Metselaar, M.Z. Jumaat, Compressive strength and microstructural analysis of fly ash/palm oil fuel ash based geopolymer mortar under elevated temperatures, Constr. Build. Mater. 65 (2014) 114–121, https://doi.org/10.1016/j.conbuildmat.2014.04.064.
[54] F. Škvára, L. Kopecký, V. Šmilauer, Z. Bittnar, Material and structural characterization of alkali activated low-calcium brown coal fly ash, J. Hazard. Mater. 168 (2–3) (2009) 711–720, https://doi.org/10.1016/j.jhazmat.2009.02.089.
[55] K. Somna, C. Jaturapitakkul, P. Kajitvichyanukul, P. Chindaprasirt, NaOH-activated ground fly ash geopolymer cured at ambient temperature, Fuel 90 (6) (2011) 2118–2124, https://doi.org/10.1016/j.fuel.2011.01.018.
[56] P. Nuaklong, K. Janprasit, P. Jongvivatsakul, Enhancement of strengths of high-calcium fly ash geopolymer containing borax with rice husk ash, J. Build. Eng. vol. 40, no. February (2021), 102762, https://doi.org/10.1016/j.jobe.2021.102762.
[57] T.W. Swaddle, Silicate complexes of aluminum(III) in aqueous systems, Coord. Chem. Rev. 219–221 (2001) 665–686, https://doi.org/10.1016/S0010-8545(01)00362-9.
[58] K. Komnitsas, D. Zaharaki, Geopolymerisation: A review and prospects for the minerals industry, Miner. Eng. 20 (14) (2007) 1261–1277, https://doi.org/10.1016/j.mineng.2007.07.011.